

## **Determination of the fraction of active inputs required by a neuron to fire.**

Guido Bugmann  
School of Computing Communication and Electronics  
University of Plymouth  
Drake Circus,  
Plymouth PL4 8 AA  
United Kingdom  
gbugmann @ plymouth.ac.uk

### **Abstract**

What fraction of the inputs to a neuron in the primary visual cortex (V1) need to be active for that neuron to reach its firing threshold? The paper describes a numerical method for estimating the selectivity of visual neurons, in terms of the required fraction of active excitatory inputs, from standard data produced by intracellular electro-physiological recordings. The method also provides an estimate of the relative strength of the feedforward inhibition in a push-pull model of the inputs to V1 simple cells. The method is tested on two V1 cells described in Carandini and Ferster (2000). The results indicate that the maximum strength of feedforward inhibition is around 30% of the maximum strength of feedforward excitation. The two V1 neurons investigated fire if more than around 40% of their excitatory LGN inputs are active.

**Keywords:** Neuronal selectivity, neuron modelling, cortical inputs modelling, visual cortex micro-circuit.

### **1. Introduction.**

The properties of neurons in the primary visual cortex (V1) are usually quantified in terms of sharpness of orientation tuning, direction selectivity, etc. How do these quantifiers translate in terms of input/output function of a spiking neuron? This paper describes a method for estimating the fraction of active excitatory inputs required by a visual neuron to fire on the basis of data on the orientation selectivity of the intracellular potential and the connectivity of V1 cells. The knowledge of this fraction is expected to help constrain computational models of neurons used in simulations, e.g. their synaptic efficacies.

If a V1 neuron only received excitatory inputs from the Lateral Geniculate Nucleus (LGN) and from other cortical cells, then the required fraction of active inputs can be determined as follows. Let us assume that, when a V1 neuron is stimulated with a drifting grating of optimal spatial frequency, speed, contrasts and orientation, all its excitatory inputs are firing at their maximum rate. These inject a maximum of current into the neuron and raise the intracellular potential to its highest value, causing a high spike firing rate. However, when the orientation of the grating is made less optimal, a smaller number of excitatory inputs become active. At a critical orientation, the current injected becomes insufficient to raise the potential to the firing threshold and the neuron ceases firing. If the rise in intracellular potential is proportional to the number of active inputs, then a comparison of the potential rise at the best stimulus orientation, with the potential rise at the threshold orientation will inform on the fraction of excitatory active inputs at the threshold.

In practice, a V1 neuron also receives inhibitory inputs and the potential is not a direct measure of the number of active excitatory inputs. Therefore, a large part of this paper is devoted to the estimation and elimination of the contribution of inhibitory inputs. Section 2 describes the model of connectivity of the LGN to V1 used in this paper. It also justifies the paper's focus on number of active inputs rather than on summed input activity. Section 3 describes the developed analytical method for estimating the relative strength of the inhibitory input. Section 4 describes how a numerical simulation to the model provides the fraction of excitatory active inputs required by a V1 neuron to fire.

## 2. Modelling the inputs to a V1 cell.

V1 neurons receive inputs from selected centre-ON and centre-OFF neurons in the LGN in such a way as to exhibit elongated receptive fields with ON and OFF areas (Hubel and Wiesel, 1962). A neuron is excited by bright spots falling in the ON area and dark spots (darker than the background illumination) falling on the OFF area. It is however inhibited by the reverse pattern of stimulation (dark on ON and bright on OFF). This is termed the push-pull mechanism. Inhibition is shown to arise via intra-cortical relay cells (Hirsch et al., 1998). Figure 1 illustrates the push-pull arrangement of inputs.

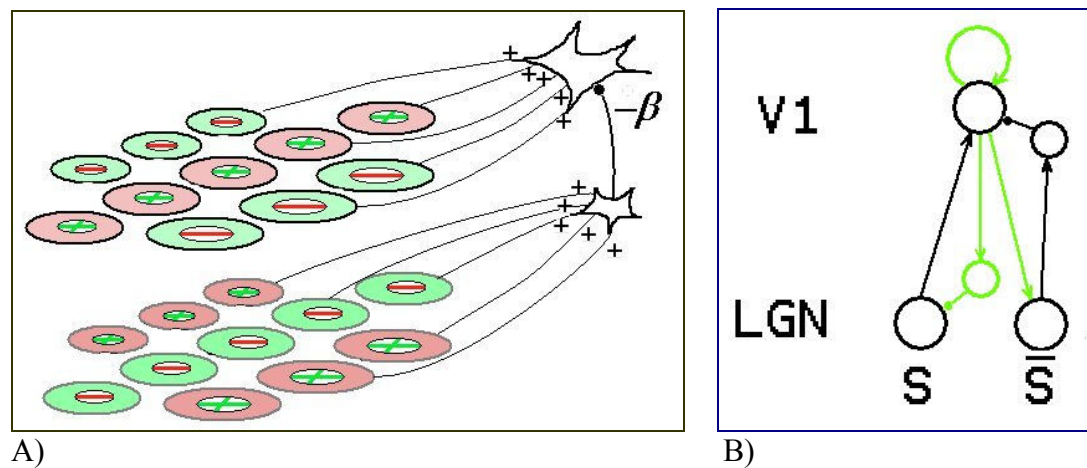


**Figure 1.** A) Push-pull arrangement of LGN inputs to V1 simple cells.  $\beta$  represents the relative strength of the inhibition. B) Diagrammatic representation of the circuit generating inputs to a V1 simple cells.  $S$  represents the preferred pattern and  $\bar{S}$  represents the opposite of that pattern.  $\bar{S}$  excites an inhibitory interneuron that inhibits the simple cell. Other feedback inputs drawn in light green are not relevant here, as the work focuses on conditions just before firing starts.

Only feed-forward (FF) connections are explicitly modelled. All feedback inputs (in green in figure 1B) are irrelevant for the question posed: For what input conditions does the neuron just start firing? V1 neurons receive significant additional cortical input. From  $\frac{1}{2}$  to  $\frac{2}{3}$  of the stimulus-driven input actually comes from intra-cortical sources (Chung and Ferster, 1998). This input has the same orientation tuning as the input from the LGN and there is no practical reason to model it here separately from

the LGN input. It is here incorporated into the LGN input. Actually, where the input comes from is irrelevant for the question posed.

In the simulation used in section 4, inputs are simulated as LGN cells of type centre-ON or centre-OFF placed randomly with a distribution given by an odd-symmetry Gabor function adapted from (Jones and Palmer, 1987) for an orientation along the y-axis (the vertical in figure 2):

$$G(x, y) = \cos\left(\frac{2\pi x}{\lambda}\right) \exp\left(-\frac{y^2}{2\sigma_y^2} - \frac{(x - x_s)^2}{2\sigma_x^2}\right) \quad (1)$$

where  $\lambda = 0.4$  (this is also the wavelength of the optimal stimulus grating),  $\sigma_x = 0.18$ ,  $x_s = 0.25 * \lambda$  (zero for even symmetry).  $\sigma_y$  is adjusted to the desired aspect ratio. To place the receptive fields (RF) centres, random (x,y) positions are picked and are kept (as opposed to rejected) with a probability given by the amplitude of the Gabor function (1). Once 40 cells have been kept, the procedure stops. The first 20 cells are assigned to the pool of cells directly exciting the V1 cell. The next 20 cells are assigned to the pool exciting the inhibitory interneuron in figure 1. The type of the cell (centre-ON or centre-OFF) is determined by the sign of the Gabor function. Figure 2 illustrates the resulting arrangement of neurons. All connection weights are equal, except for the one between the inhibitory interneuron and the V1 cell, set to  $-\beta$ . Only input currents are of interest here. Firing is not simulated.

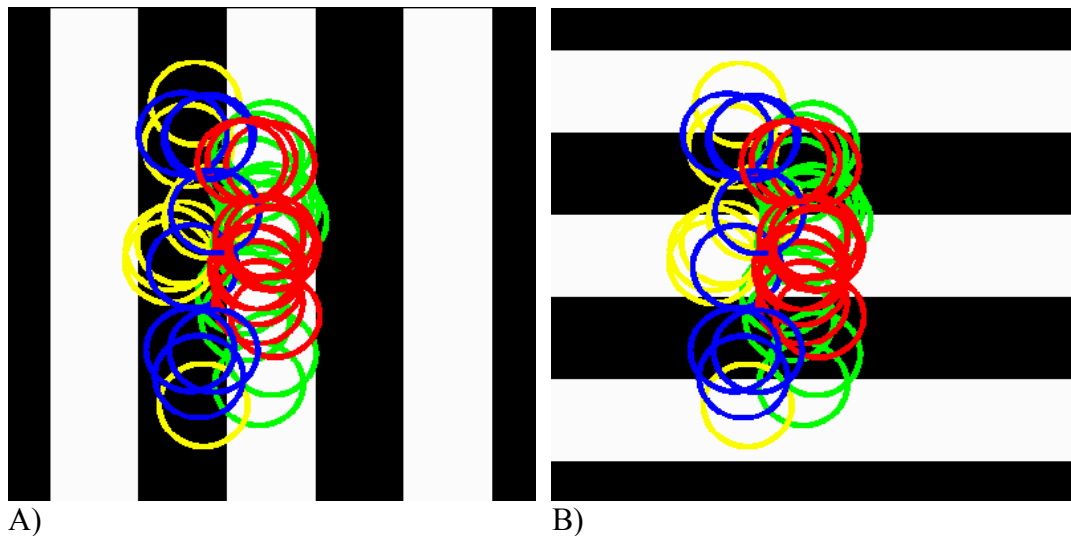


**Figure 2:** Spatial arrangement of LGN cells feeding into a V1 simple cell. The central part of the LGN Receptive fields (RF)s is indicated by colored circles. The pool of 20 direct excitatory inputs is represented by red (centre-ON) and blue (centre-OFF) circles. The pool of 20 inputs feeding into the inhibitory interneuron is represented by yellow (centre-ON) and green (centre-OFF) circles. Note the opposite phase of the spatial location of the inputs to the interneuron. The black and white stripes exemplify the stimulus used in numerical simulations. A) Optimal orientation. B) Worst orientation.

The response of LGN cells to a visual stimulus are approximated by the standard Difference-of-Gaussians (DOG) function (see e.g. Archie and Mel, 2000), limited to a radius of 3 half-width of the central Gaussian.

The results presented in following section are based on the assumption of a proportional relation between number of active inputs and potential rise. This can be justified in a two-step argument. The first step deals with the concept of "number" of active inputs. Previous work has shown that short-term synaptic depression can have the effect of "binarizing" the post-synaptic effect of input spike trains (Bugmann, 2002). In practice, this means that, above a given input firing rate, the input current seen by the post-synaptic neuron is a constant independent on the input firing rate. Thus, the total post-synaptic current is essentially a measure of the number of active inputs, not of their summed firing frequencies. Computationally, it makes sense for a visual neuron to decide whether a preferred pattern is seen on the basis of the number of elementary features present rather than their intensity (contrast invariance). Note that recent data shed doubts on the standard views on synaptic depression (Boudreau and Ferster, 2005), which may however be offset by findings on the saturation of LGN response (Ferster, private communication). In any case, the binary nature of stimuli generally used leads to a bimodal distribution of strengths of LGN responses (not shown here) justifying the discussion of inputs in terms of numbers rather than summed activities. The second step deals with the linear relation between input current and membrane potential. This is a generally accepted approximation. For instance, in the leaky-integrate-and fire model of a neuron the steady-state potential  $V$  is the product of the leak resistance  $R$  and the input current  $I$  ( $V=RI$ ). However, there may be a question about the effect of spikes firing and reset mechanisms on the maximum measured potential. Although experimental data show that the potential of a strongly stimulated cell can exceed the firing threshold, there is also evidence that the firing threshold has an "capping" effect on the potential (see e.g. figure 1 in Carandini and Ferster, 2000). This effect, however, is not too critical here, as the work focuses on input conditions that bring the neuron near to the firing threshold. The analysis of experimental data in following sections however will require some care.

### 3. Estimation of the relative strength of inhibition.

This section explains how it is possible to estimate the value of  $\beta$  from response data published in Carandini and Ferster (2000) –henceforth abbreviated as C&F - by assuming the simple model in figure 1B. When a grating stimulus made of dark and bright bars is moved over the receptive field, it successively activates and inhibits the V1 cell. If the grating has the optimal orientation and is moved at the optimal speed, the cell will fire strongly during the phases of excitation (C&F)<sup>1</sup> and will strongly be inhibited one half cycle later. Figure 3 shows an example of total input current into the V1 simple cell when the grating is moved across the RF. If one assumes that the potential of the soma is proportional to the input current, then figure 3 also shows the intracellular potential that could be recorded from the cell. At phase zero only the excitatory inputs are active and, at phase 180 deg., only inhibitory inputs are active. Thus, the ratio from  $V_-$  to  $V_+$  in figure 3 is a measure of the relative strength of inhibition  $\beta$ :

---

<sup>1</sup> At the optimal speed, it is likely that inhibitory rebound also contributes to the spiking and the value of  $V_{max}$  in figure 3.

$$\beta = \frac{V_-}{V_+} \quad (2)$$

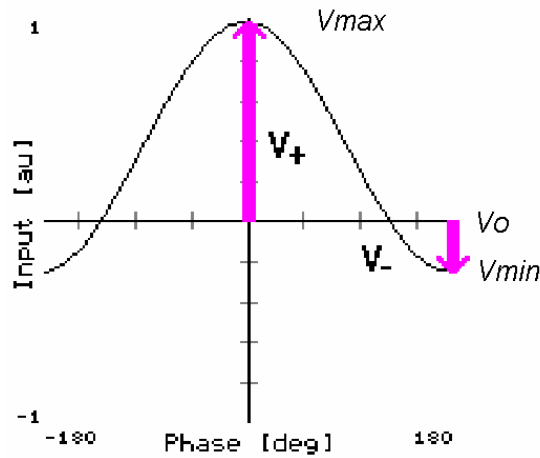


**Figure 3.** Example of total input current into the V1 simple cell when the grating is moved across the RF defined by the LGN cells in figure 2. At phase zero only the excitatory inputs are active and, at phase 180 deg., only inhibitory inputs are active. The figure represents interchangeably the input current or the intracellular potential.

Experimentally,  $V_+$  cannot exactly be determined, as the neuron tends to spike before the maximum potential  $V_+$  is reached. Both  $V_+$  and  $V_-$  are limited by the reversal potentials of their respective ionic channels. Nevertheless, one can explore if meaningful estimates can be made from experimental data. C&F provide data on the "modulation"  $M$  of the cell's potential by the drifting grating. This is the peak-to-peak amplitude of the sinusoidal curve that best fits recordings. We will assume that

$$M = Vmax - Vmin \quad (3)$$

C&F also provide the mean value of the potential  $Vav$  and an indication of the resting potential of the cell  $Vo$ . Given that

$$Vav = \frac{1}{2}(Vmax+Vmin) \quad (4)$$

$$V_- = Vo - Vmin \quad (5)$$

$$V_+ = Vmax - Vo \quad (6)$$

the expression (2) for  $\beta$  becomes:

$$\beta = \frac{Vo - Vav + \frac{1}{2}M}{Vav + \frac{1}{2}M - Vo} \quad (7)$$

Applying formula (7) to cells 61 and 71 in figures 4 and 6 of C&F, one finds  $\beta = 0.34$  and 0.29 respectively (see table 1). Note that both  $M$  and  $Vav$  are probably

underestimates due to the capping of  $V_{max}$ . Thus, formula (7) is likely to overestimate  $\beta$ . A better estimation could be produced with data obtained with a stimulus with the ideal spatial frequency and orientation, but that activates less LGN cells, e.g. being shorter, or sparser, so that the V1 simple cell does not reach its firing threshold.

Cell	$V_o$ [mV]	$M$ [mV]	$V_{av}$ [mV]	$\beta$
61	-76	19.3	-71.3	0.34
71	-73.4	21.0	-67.6	0.29

**Table 1:** Experimental data  $V_o$ ,  $M$  and  $V_{av}$  on cells 61 and 71 estimated from figure 4 and figure 6 in C&F and corresponding  $\beta$  values calculated using (7). The experimental values come from the smoothed curves in C&F at the optimal orientation. Very similar values are obtained from the raw experimental points (e.g. fig. 1&2 in C&F).

#### 4. Estimating the necessary fraction of active inputs.

To estimate the necessary fraction of active inputs, one needs to know the contribution of excitatory and inhibitory inputs in conditions where V1 neurons barely respond. Such conditions are regularly generated during measurements of orientation tuning curves. Given that a V1 neuron only fires when the drifting grating is presented close to the optimal phase, this section will focus input conditions at the optimal phase when the orientation of the stimulus is varied.

During measurements of orientation tuning curves, both excitation and inhibition are active in varying proportions. When the stimulus has the optimal orientation, no LGN cells in the inhibitory pool sees its best stimulus, but all cells in the excitatory pool are optimally stimulated. This is the case in figure 2A where all red centre-ON cells have a bright stimulus on their centre and all blue centre-OFF cells have a dark stimulus on their centre. When the stimulus is at the orientation perpendicular to the optimal one, only some LGN in the excitatory pool see their best stimulus. In addition, some cells in the inhibitory pool can now see good stimuli, for instance, some yellow centre-ON cells in figure 2B. Thus, the inhibitory contribution increases as the orientation becomes less optimal.

To estimate the fraction of excitation and inhibition at the threshold orientation, numerical simulations are use here. Such simulations require an indication of the aspect ratio of the pools in LGN for the generation of the positions of the RFs of the LGN cells (as described in section 2). No information on aspect ratios is provided in C&F and a wide range of aspect ratio values have been reported in the literature (Gardner et al., 1999; Pei et al., 1994). However, these can be estimated through fitting the model to the data. In the simulation, a distribution is generated with a given aspect ratio, then the positions are stretched or compressed vertically (in figure 2) until the best match is achieved with experimental orientation tuning curves of the intracellular potential at the best phase. These curves are not directly found in C&F. However, from the published data on modulation, average potential and resting potential, one can determine the maximum potential increase achieved by the V1 cell at the optimal phase for each orientation  $\alpha$ :

$$V_{max}(\alpha) = V_{av}(\alpha) + 1/2 M(\alpha) - V_o \quad (8)$$

Experimental values are available for deviations  $\alpha$  from the preferred orientations increasing in steps of 30 degrees. Figure 4 shows the calculated  $V_{max}(\alpha)$  data for two cells and the best fit obtained from the model. The quality of fit and the best-fit parameter values (Table 2) depend on the initial random distribution of RF centres of LGN cells. When only distributions leading to relatively symmetrical orientation tuning curves are used for fitting, the parameter values obtained were reproducible within a few percents.

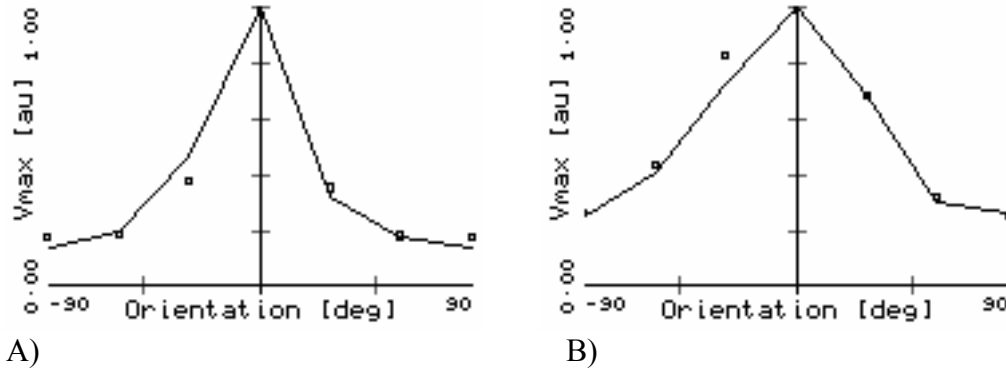


**Figure 4.** A) cell 61. B) Cell 71. The square symbols show the values of  $V_{max}(\alpha)$  calculated using (8) from smoothed data from figures 4 and 6 in C&F. The continuous lines link the values produced by the simulated V1 cell using the model in section 2. The fit was constrained by the  $V_{max}(\alpha)$  values for only positive values of angles, to reduce computing time. The potentials are normalized to 1 for the best orientation adjusted to zero in both cells.

Cell	Threshold angle $\alpha_{th}$ [deg]	Aspect ratio	$\beta$ from fit (from 7)	$F_+$ ( $\alpha_{th}$ )	$F_-$ ( $\alpha_{th}$ )	$F_{net}$ ( $\alpha_{th}$ )
61	30	4.97	0.26 (0.34)	0.35	0.03	0.32
71	75	3.09	0.26 (0.29)	0.45	0.10	0.35

**Table 2.** Results of model fitting. The threshold angle  $\alpha_{th}$  is the maximum deviation allowed from the preferred orientation before the two indicated neurons stop firing. This is estimated from figures 4 and 6 in C&F. The aspect ratio and  $\beta$  are values obtained from fitting the model to the data, as shown in figure 4. The values  $F_+$ ,  $F_-$  and  $F_{net}$  are input currents described in the text. They are obtained by running simulations at the threshold angles of each cell.

Using the parameters of best fit, one can run the simulation for the particular threshold angle of difference to the preferred orientation. This simulation informs on the proportion  $F_+$  and  $F_-$  of excitatory and inhibitory input currents at that orientation

$$F_+ = I_+ / I_{max} \quad (9)$$

$$F_- = I_- / I_{max} \quad (10)$$

Where  $I_{max}$  is the current generated by the stimulus at the best orientation (set to zero in all cells). Note that the  $I_-$  is the current reaching the V1 cell and includes the modulation by  $\beta$ .

$$I_{max} = I_+(\alpha = 0) \quad (11)$$

From this one can calculate the fraction  $F_{net}$  of net input current relative to the maximum current.

$$F_{net} = (I_+ - I_-)/I_{max} = F_+ - F_- \quad (12)$$

Values of  $F_{net}$  are the normalised potentials plotted as continuous lines in figure 4.

The fraction  $F_{net}$  represents the fraction of excitatory LGN inputs that would need to be active if no inhibition were present. This is a measure of the true selectivity of the V1 cell. The fraction  $F_+$  is the larger fraction of LGN cells in the excitatory pool that need to be active to make the V1 neuron fire in the presence of inhibition. This is a measure of the selectivity of the push-pull circuit.

One sees for the two example cells investigated here, that the V1 cells are intrinsically moderately selective, requiring approximately 32%-35% of active inputs to fire. The push-pull circuit is slightly more selective, requiring 35%-45% of active inputs.

Again caution is needed due to a probable underestimation of  $V_{max}$  in (8) due to a capping of potentials by firing mechanisms. As this affects relatively more the high-potential situations, the curves in figure 4 would have had a narrower peak and lower tails. Exploratory work indicates that this would have led to higher values of  $\beta$  and  $F_+$  and little changes in  $F_{net}$ .

In summary, the proposed formula (7) probably overestimates  $\beta$ . The fitting procedure on the other hand, is likely to underestimate  $\beta$ . This is reflected in the results in table 2. It is encouraging to see that the resulting range of possible values is nevertheless narrow, pointing to values around 30% of relative strength of inhibition.

The selectivities of the two V1 cells used in this study are relatively low, either individually, or as part of the push-pull circuit. This may be particular to these cells that possibly are not representative of the population of V1 cells. In V1 cells, firing generally starts at the half height of the average potential tuning curve (C&F, Pei et al., 1994). However, in the two cells considered here, firing already starts in the lower third of the curve (although here  $V_{max}$  curves are used instead of average potential curves).

## 5. Conclusion

The paper has described a numerical method for estimating the selectivity of visual neurons in terms of the required fraction of active excitatory inputs, from standard data produced by intracellular electro-physiological recordings. The method also provides an estimate of the relative strength of the feedforward inhibition in a push-pull model of the inputs to V1 simple cells. The method has been tested on two V1

cells assumed to be part of a push-pull circuit. These cells experience around 30% of relative feedforward inhibition and fire only if more than around 40% of their excitatory LGN inputs are active. This is still exploratory work. Several questions about the approximations made need careful investigation. Applications to more representative cells would be useful, especially if measurements are done in conditions closer to the domain of validity of this method.

## References.

Archie K.A. and Mel B.W. (2000) A model for intradendritic computation of binocular disparity. *Nature Neuroscience*, 3:1, p. 54-63.

Boudreau C. E. and Ferster D. (2005) Short-Term Depression in Thalamocortical Synapses of Cat Primary Visual Cortex. *The Journal of Neuroscience*, 25:31, pp.7179 –7190.

Bugmann G. (2002) Synaptic depression increases the selectivity of a neuron to its preferred pattern and binarizes the neural code. *Biosystems: Special Issue on Neural Coding*, 67, 17-26.

Carandini M. and Ferster D. (2000) Membrane potential and firing rate in cat primary visual cortex. *J. of Neuroscience*, 20:470-484.

Chung S. and Ferster D. (1998) Strength and orientation tuning of the thalamic input to simple cells revealed by electrically evoked cortical suppression. *Neuron*, 20: 1177-1189.

Gardner J.L., Anzai A., Ohzawa I., and Freeman R. (1999) Linear and nonlinear contributions to orientation tuning of simple cells in the cat's striate cortex. *Visual Neuroscience* 16: 1115-1121.

Jones J.P. and Palmer L.A. (1987) An evaluation of the two-dimensional Gabor filter model of simple receptive fields in cat striate cortex. *J. Neurophysiology*, 58:1233-1258.

Hirsh J.A., Alonso J.-M., Reid R.C. and Martinez L.M. (1998) Synaptic Integration in Striatum Cortical Simple Cells. *The journal of Neuroscience*, 18:22, pp. 9517-9528.

Hubel D.H. and Wiesel T.N (1962) Receptive fields, binocular interaction and functional architecture in the cat visual cortex. *J. Physiol. (London)*, 160:106-154.

Pei X., Vidyasagar TR, Volgushev M, Creutzfeldt OD (1994) Receptive field analysis and orientation selectivity of postsynaptic potentials of simple cells in cat visual cortex. *The Journal of Neuroscience*, 14:7130-7140.